Bull. Soc. Photogr. Imag. Japan. (2015) Vol. 25 No. 2: 25–30

Original Paper

Simulating Gloss of Curved Paper by Using the Point Spread Function of Specular Reflection

Norimichi Tsumura*, Kaori Baba*, and Shinichi Inoue**

Abstract: We propose a method that uses the point spread function of specular reflection (SR-PSF) to simulate paper gloss. The SR-PSF is defined as the impulse response of specular reflection, which is the distribution of light intensity reflected from microscopic facets on the surface of the paper. In this study, we used a flat sample holder and measured the SR-PSFs of six paper samples, each of which had a different level of specular gloss. We then used two different methods based on the measured SR-PSFs to simulate the gloss of curved paper. The results show that the gloss of curved paper can be adequately simulated by using the measured SR-PSF of that paper.

Key words: paper gloss, specular reflection, point spread function, reproduction

1. Introduction

Gloss is an important quality of printing paper, and during the manufacturing process, the gloss (i.e., the sharpness of a reflected light source on the surface) of the curved paper is tested visually. Gloss is a specular reflection phenomenon in the field of optics. Hunter and Harold summarize the results of many different materials and their glossiness rankings, and showed the six different criteria by which glossiness rankings are made [1]. Their types of gloss are specular gloss, sheen, contrast gloss, absence of bloom gloss, distinctness of image gloss and surface uniformity gloss. In this paper, we focus on the specular gloss and distinctness of image gloss since the gloss of paper is mainly dominated by these two attributes.

Many reflection models have been proposed and are used in computer graphics software to simulate gloss [2-7]. Technologies that can measure and characterize gloss based on the measured bidirectional reflectance distribution function have been developed and used in evaluations [6-16]. However, most of them require long measurement times and many images of the surface of the target object. We therefore assessed technologies for measuring gloss, particularly on paper, as a point spread function of specular reflection (SR-PSF) [14-16]. The SR-PSF can be measured from a single image of the spread of specular reflection on the target paper.

In this paper, we propose a new method, which is not based on conventional reflection models, that uses the SR-PSF to simulate the gloss on the surface of a curved paper. The SR-PSF is defined as the impulse response of specular reflection. The conventional PSF is used as a transfer function in image science [17], and it can be calculated from the modulation transfer function (MTF). There have been some studies of the MTFs of diffuse reflections [18, 19], including one

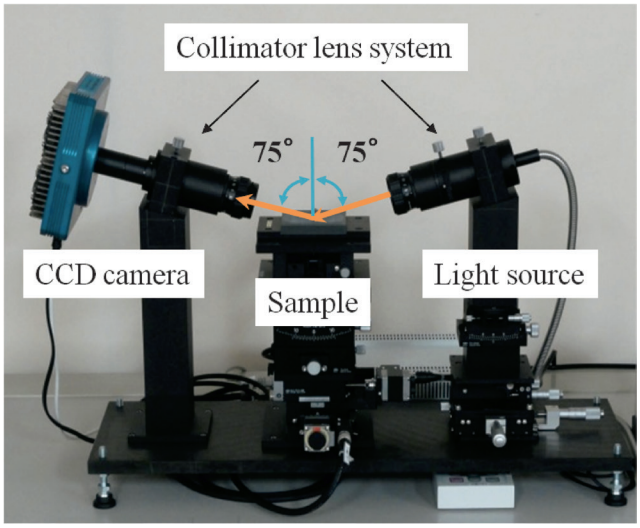

Figure 1 The apparatus for measuring the SR-PSF

Received: 19th, June 2015; Accepted: 15st, September 2015

*Department of Information and Image Sciences, Chiba University, CHIBA, JAPAN
**Mitsubishi Paper Mills Limited, TOKYO, JAPAN

by the authors of this paper [18]. The SR-PSF is an expansion of the conventional PSF for diffuse reflections into the specular reflection on the surface of paper [14-16].

In the next section, we introduce a method for measuring the SR-PSF of paper. In Section 3, we present the measurements that we used for the simulations. Two methods to simulate paper gloss are proposed, and the results of the simulations are shown and discussed. We present our conclusions in Section 4.

2. Experiment

Point spread function of specular reflection (SR-PSF) [14-16] can be measured from a single image of the spread of specular reflection on the target paper. This PSF is different from conventional PSF of optical system. Conventional PSF is measured on the imagining plane as the spread of point, but SR-PSF is defined in the following collimator lens system. Figure 1 shows the apparatus that we used to measure the SR-PSF for the study presented in this paper. It was developed by one of the authors [14-16]. Light from a pinhole light source is projected onto a sample paper through a collimator lens system. The light reflected from the sample paper is focused, and a two-dimensional charge-coupled device (CCD) camera captures a digital image of the intensity distribution of the reflected light. The captured image of the intensity distribution shows the SR-PSF of the paper sample because it is an impulse response to the pinhole light. The lighting and viewing angles were both set to be 75°, according to the standard method (as defined by the ISO [21]) for measuring the specular gloss of paper. In this apparatus, the pinhole is made of a metal plate, and its diameter is 100 μm. The CCD camera has 512×512 pixels, and it has an output level of 16 bits per pixel. In the captured image, each pixel corresponds to 0.029 mm on the sample. The output values could be used as a measure of the light intensity because we confirmed in advance that there was a linear relationship between them. Each paper sample was set on the sample bed, and the SR-PSF was measured in a darkroom. We can ignore the diffuse reflection component in this geometry since the value of reflected specular reflection is strongly higher than diffuse reflection. We also prepared and measured a sample of black glass with a refractive index of 1.567, which was used to perform the alignment of the optical system by setting the SR-PSF for the black glass is similar to the delta function.

To define the SR-PSF, we considered both macroscopic and microscopic facets, as shown in Figure 2. The macroscopic facets produce the visible curvature of the surface, and the microscopic facets produce the lobe of the specular reflection. In this system for measuring the SR-PSF, since the angle of the macroscopic facet is fixed and the paper is attached to a flat bed, the directions of the reflected lights are determined by the angles of the microscopic facets of the paper. Therefore, the distribution of the reflected light intensity results in the gloss on the paper, as measured by the SR-PSF that is an impulse response to the pinhole light. In Figure 2, we define the angles of the macroscopic and microscopic facets as $(\theta x, \theta y)$ and $(\theta x', \theta y')$, respectively. In the actual measurements, the angle of the macroscopic facet was set to (0°, 0°), since the paper was placed on a flat bed.

Six types of samples, each with a different level of specular gloss, were prepared from the same type of paper. Figure 3 shows the specular gloss, as measured by a gloss meter (GM-26PRO, Murakami Color Research Laboratory), following a standardized procedure (ISO 8254-1:2009) [20]. Figure 4 shows the SR-PSF values that were measured by using the apparatus shown in Figure 1. The x' and y' axes indicate the position of the pixel on image from the CCD camera. The z' axis indicates the value output by the CCD camera. As the specular gloss of the sample paper decreases, the measured SR-PSF has a broader distribution, and the peak value of the SR-PSF

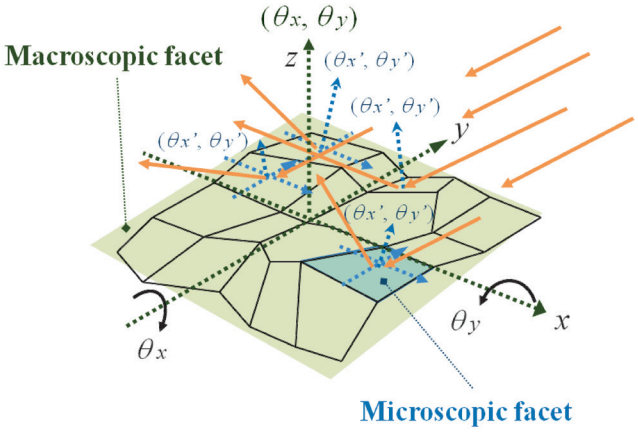

Figure 2 Schematic diagram showing the macroscopic and microscopic facets on a flat paper surface

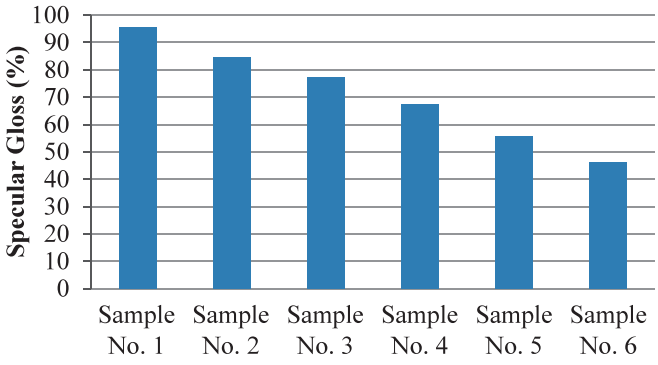

Figure 3 Specular gloss of the sample papers used in this study

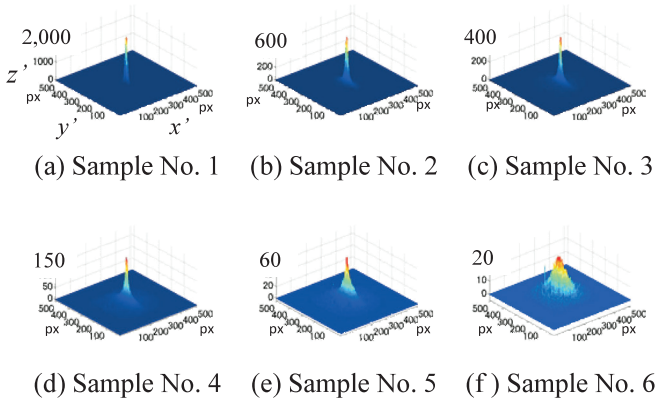

Figure 4 Measurements of the SR-PSFs.
The maximum value on the z'-axis was (a) 2000, (b) 600, (c) 400, (d) 150, (e) 60, and (f) 20.

Table 1. Specifications of the imaging device used in this study

Camera	Nikon D3X
Lens	Nikon AF MICRO NIKKOR 60mm 1:2.8 D
Polarizing filter	Nikon 62 SPL 2 62mm
Shutter speed (sec)	1.6
F-number	32
ISO speed (sec)	200

decreases with decreasing specular gloss. It is difficult to estimate the shape of SR-PSF for the measured specular gloss. Then, it is required to measure the SR-PSF or propose the shape of SR-PSF to give expected gloss on paper for printing industries as is mentioned in beginning of the next section.

3. Simulating the gloss on curved paper

3.1 Method

In the paper and printing industries, the gloss of paper is usually observed by the curved paper. Therefore, it is expected to develop the simulator for reproducing the appearance of gloss on the curved paper for acceleration of product development. Figure 5 shows a diagram of the methodology for simulating gloss on paper. First, a fluorescent light was projected onto a cylindrically curved specular object (of diameter 260 mm) in order to obtain an initial image. The image function $f_{mirror}(x', y')$ was used to express the image of the object. Since the fluorescent light is not the pinhole, $f_{mirror}(x', y')$ is different from the SR-PSF of black glass. The size of $f_{mirror}(x', y')$ was 1512×1008 pixels, and at the center of the image, each pixel corresponds to 0.029 mm on the object; this resolution matches that of the SR-PSF. Table 1 summarizes the specifications of the photographing device used in this study.

In this section, we discuss the two methods used to simulate the gloss on paper. In Section 3.2 (i), we introduce the convolution method, and in Section 3.2 (ii), we introduce the kernel method. We note that, for both methods, we normalized the measured SR-PSFs (shown in Figure 4) according to the specular gloss, so that the value of the pixel for each SR-PSF corresponded to the reflectance.

(i) Convolution method

In the first method, we performed a convolution between the SR-PSF $f_{SR\text{-}PSF}(x', y')$ and the original image $f_{mirror}(x', y')$, as follows.

$$f_{specular}(x', y') = \iint f_{mirror}(x'', y'') f_{SR\text{-}PSF}(x'-x'', y'-y'')dx''dy'' \quad \ldots(1)$$

The SR-PSF $f_{SR\text{-}PSF}(x', y')$ was measured by the method shown in the previous section. As was mentioned above, the image function $f_{mirror}(x', y')$ was an image of mirror –like cylindrically curved object as is shown in the top of Fig. 5. Then, the convolution between an image of mirror-like object and SR-PSF will give us the simulated gloss appearance. Here, it is noted that $f_{mirror}(x', y')$ and SR-PSF $f_{SR\text{-}PSF}(x', y')$ are known function, and $f_{specular}$ is the estimated function used as the predicted appearance. It is also noted that convolution operation is shift invariant operation, then SR-PSF $f_{SR\text{-}PSF}(x', y')$ is same at each position even if the curved area.

Next, we added the calculated $f_{specular}(x', y')$ to the diffuse image of

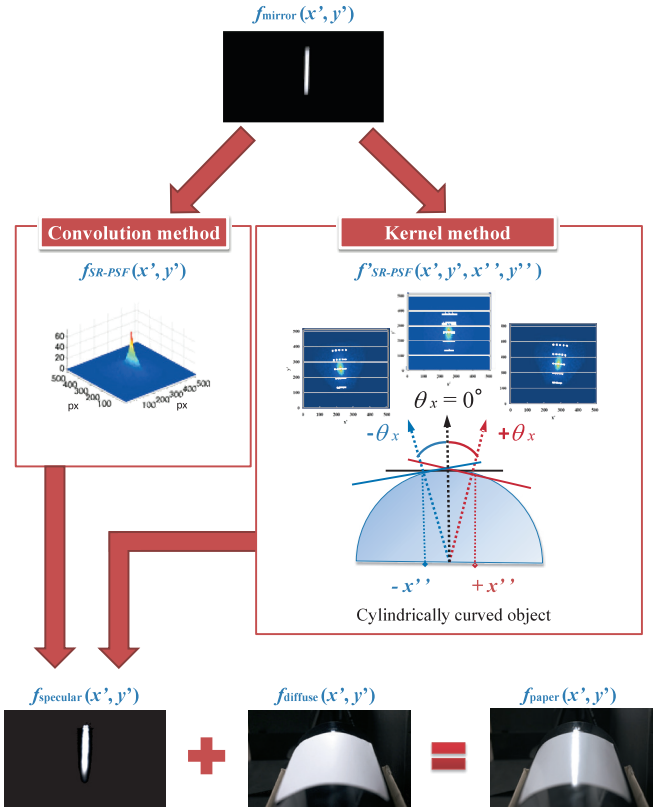

Figure 5 Methodology used to simulate gloss on paper

the paper $f_{diffuse}(x', y')$. This diffuse image was captured by setting the polarizing filter in front of the light source and camera with the crossed Nicols arrangement, so that the gloss component was removed. We note that the paper sample was attached to a cylindrically curved object. The final process required to obtain the simulated gloss for the curved sample paper is shown in Eq. (2).

$$f_{paper}(x', y') = f_{specular}(x', y') + f_{diffuse}(x', y') \quad \ldots(2)$$

In Eq. (2), we assumed that the imaging system for observation has enough length of depth of focus to ignore the PSF of the imaging system toward the light source in the experiment. We also assumed that the reflection model can be described by dichromatic reflection model.

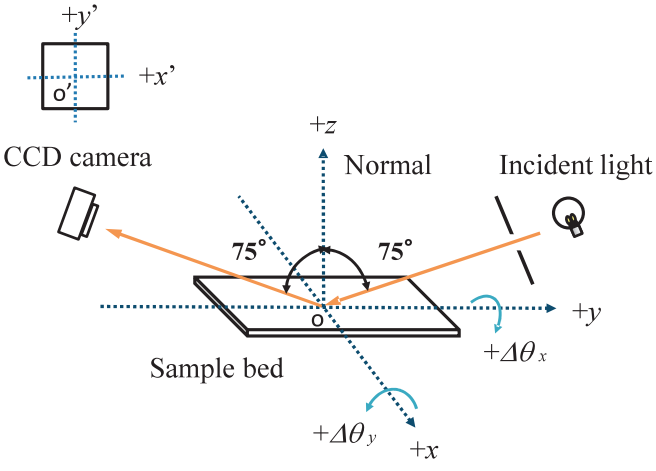

Figure 6 Coordinate system of the apparatus used to measure the SR-PSF

(ii) Kernel method

In the second method, we performed a kernel operation between the transformed SR-PSF $f'_{\text{SR-PSF}}(x', y', x, y)$ and the original image $f_{\text{mirror}}(x', y')$, as follows.

$$f_{\text{specular}}(x', y') = \iint f_{\text{mirror}}(x'', y'') f'_{\text{SR-PSF}}(x', y', x'', y'') dx'' dy'' \quad \ldots(3)$$

Here, $f'_{\text{SR-PSF}}(x', y', x'', y'')$ is obtained by transforming the original SR-PSF $f_{\text{SR-PSF}}(x', y')$ as a function of the angle of the cylindrically curved specular object. It is noted that the Kernel operation can be used for shift variant operation, then $f'_{\text{SR-PSF}}(x', y', x'', y'')$ can be varied with the change of angle of the curved specular object. In the following paragraph, we will explain this transformation process.

In the measurement apparatus (Figure 1), the collimator lens system focuses the incoming parallel light rays onto a single point on the CCD. Even though the light rays are parallel when they enter the measurement apparatus, they reach different points on the CCD. This is because, as shown in Figure 2, the angles of the microscopic facets (θ_x', θ_y') vary, and so the angles of the light rays are changed when they are reflected from the paper. Figure 6 shows the three-dimensional coordinate system of the measurement apparatus, where the angle of the macroscopic facet (θ_x, θ_y) is set to (0°, 0°). The angles of (θ_x, θ_y) are used to indicate the slope of curved paper. A light ray reflected from a microscopic facet with an angle of (θ_x', θ_y') is observed at the position (x, y, z), where y is the optical axis, x is perpendicular to y and lies in the plane of the sample bed, and z is normal to the plane of the sample bed. The position (x, y, z) is calculated as shown here.

$$\begin{pmatrix} x \\ y \\ z \end{pmatrix} = d \begin{pmatrix} \sin(2(\theta_x, \theta_x')) \cos(75^\circ + 2(\theta_y + \theta_y')) \\ \sin(75^\circ + 2(\theta_y + \theta_y')) \\ \cos(2(\theta_x + \theta_x')) \cos(75^\circ + 2(\theta_y + \theta_y')) \end{pmatrix} \quad \ldots(4)$$

Here, d is the distance between the center of ample and center of CCD. The CCD camera angle was fixed at 75 degrees. In this equation, position O is only considered on the sample. It can be said that the ray from different position of sample also give the same results since the sample is illuminated collimated parallel light and reflected light is observed by the focused point. The new coordinate system corresponding to the CCD camera is defined by (x', y', z'). The position (x', y') of the pixel in the image of the CCD camera was calculated by rotating the original position vector, as follows.

$$\begin{pmatrix} x' \\ y' \\ z' \end{pmatrix} = \begin{pmatrix} 1 & 0 & 0 \\ 0 & \cos(75^\circ) & \sin(75^\circ) \\ 0 & -\sin(75^\circ) & \cos(75^\circ) \end{pmatrix} \left\{ \begin{pmatrix} x \\ y \\ z \end{pmatrix} - d \begin{pmatrix} 0 \\ \sin(75^\circ) \\ \cos(75^\circ) \end{pmatrix} \right\} \quad \ldots(5)$$

In this equation, rotated axis is x-axis in the Figure 6 to give the sensor image coordinate. When the angles of the macroscopic facets (θ_x, θ_y) are changed, the pixel positions that correspond to each angle of the microscopic facets (θ_x', θ_y') can be calculated by using Eqs. (4) and (5). Therefore, with Eqs. (4) and (5), we can transform the SR-PSF measured at $(\theta_x, \theta_y) = (0°, 0°)$ to that measured at $(\theta_x, \theta_y) = (\Delta\theta_x, \Delta\theta_y)$. In this paper, we will only consider a rotation of $\Delta\theta_x$, since, with a cylindrically curved object, the paper is only bent in the θ_x direction. This geometry is the form most commonly used to evaluate the gloss of paper.

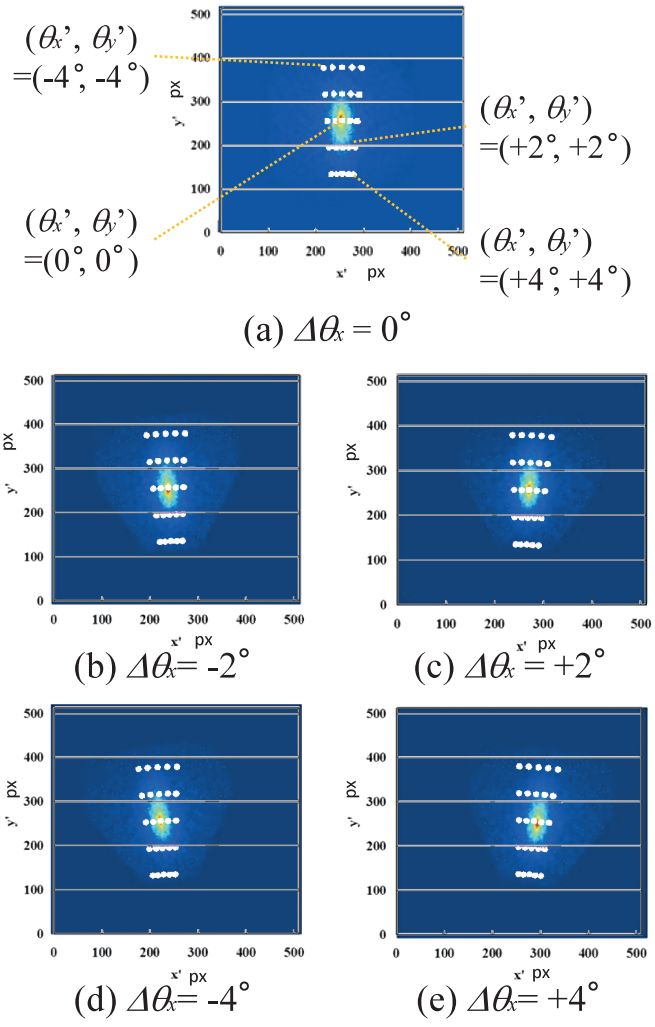

Figure 7 The transformed SR-PSFs for sample No. 5.
The values of angle $\Delta\theta_x$ were (a) 0°, (b) -2°, (c) +2°, (d) -4°, and (e) +4°.

As an example of the transformed SR-PSF, Figure 7 shows the results for sample No. 5 in Figure 4(e). Figure 7(a) shows the measured SR-PSF for $(\theta_x, \theta_y) = (0°, 0°)$. Figures 7(b) to 7(e) show the transformed SR-PSFs as a function of $\Delta\theta_x$, where $(\theta_x, \theta_y) = (\Delta\theta_x, 0°)$, for $-4° \le \Delta\theta_x \le +4°$, at intervals of 2°. The white dots in Figure 7 show the (x', y') that corresponds to the angle of the microscopic facets (θ_x', θ_y'), where $-4° \le \theta_x', \theta_y' \le +4°$, at intervals of 2°. This transformation can be considered as rotation for y-axis in 3 dimensional space. These are examples of the transformed SR-PSF, practical application will be given in the next section by comparing the captured images.

3.2 Results of gloss simulation

As was mentioned before, in the paper and printing industries, the gloss of paper is usually observed by the curved paper. Therefore, it is expected to develop the simulator for reproducing the appearance of gloss on the curved paper for acceleration of product development. In this sub-section, we will compare between the results of gloss simulation and real appearance. Figure 8 shows the images that resulted from simulating the gloss for six kinds of paper. In these figures, a logarithmic conversion was applied to the values of $f_{\text{paper}}(x', y')$ because they were too dark to observe with a low-dynamic-range

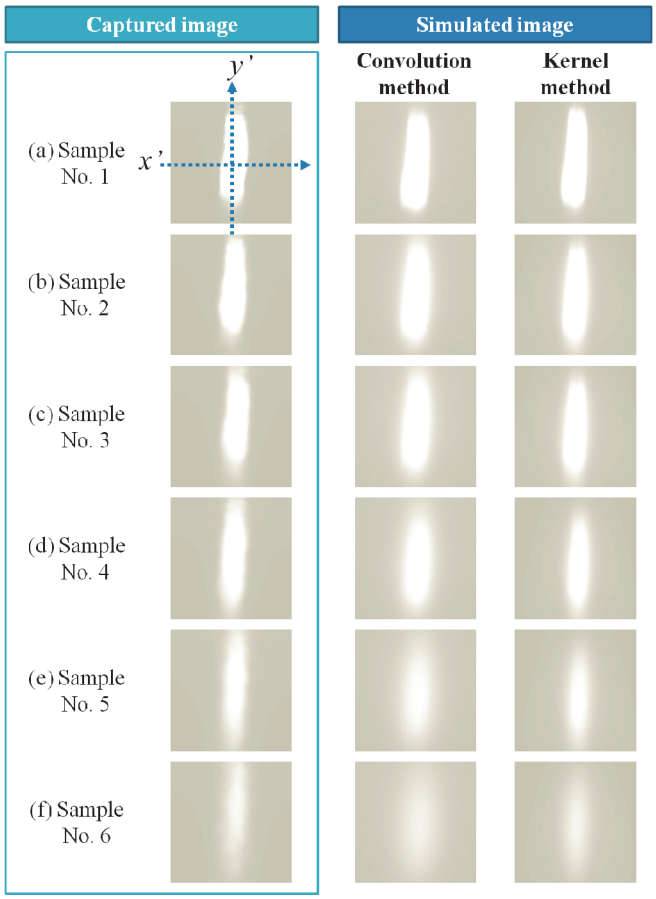

Figure 8 Simulations of gloss on paper.
From left to right, the figures show the captured images, the images simulated by using the convolution method, and the images simulated by using the kernel method.

display. The figures on the left side, center, and right side show, respectively, the images of the real gloss, as captured by the camera, and the simulated gloss from the convolution and kernel methods. Figure 9 shows the pixel values for the x' direction for each image in Figure 8. These pixel values were obtained by averaging the pixel values for the y' direction; the values shown are the initial values before the logarithmic conversion. By comparing the distributions of the captured images to those of the simulated images, it can be seen that the gloss on the curved paper was simulated adequately for most of the samples. In all cases, the kernel method simulated the captured image better than did the convolution method. Figure 10 shows the half width at half maximum (HWHM) for each distribution of the pixel values shown in Figure 9. It is noted that the advantages of the kernel method can be seen particularly in Samples No. 4, No. 5, and No. 6, where the surface gloss is lower than it is in the other samples. We also performed the subjective evaluation for 6 subject. All subjects answered that the all images by Kernel method is similar to the captured images compared with the images by convolution method. These results indicate that the transformation of SR-PSF $f_{\text{SR-PSF}}(x', y')$ into $f'_{\text{SR-PSF}}(x', y', x'', y'')$ is effective for simulating gloss.

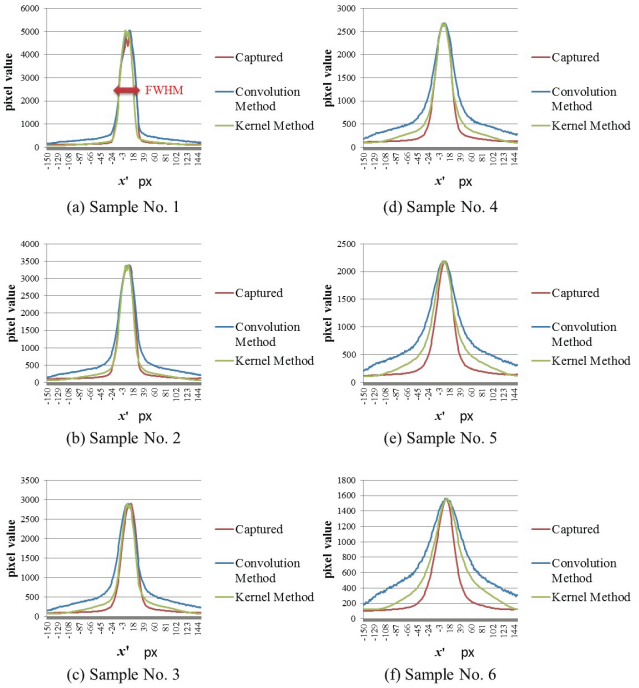

Figure 9 The values of the pixels in the x' direction for each image in Figure 8

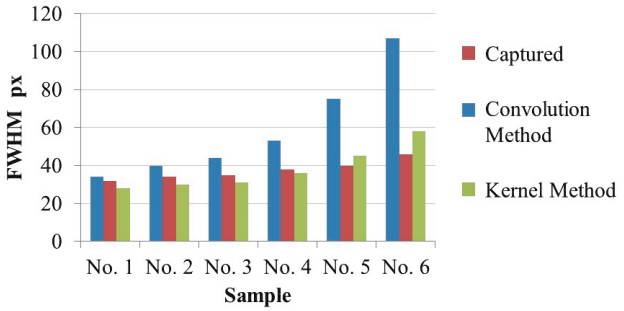

Figure 10 The half width at half maximum (HWHM) for each distribution of pixel values shown in Figure 9

4. Conclusion

We measured the SR-PSFs of six paper samples, each of which had a different level of specular gloss, and we then simulated the gloss intensity distribution by using the convolution and kernel methods, both of which were based on the SR-PSF for an original image of a cylindrically curved object with mirror-like reflection. From the simulated results, we found that both methods are able to adequately simulate the gloss on paper, and that the kernel method better simulates paper with low gloss.

In the micro facets, the shadowing and masking of facets cause off-specular phenomena as in Torrance and Sparrow model2. In this paper we ignore this phenomena. We need to consider this phenomena when the incident angle increases. We also need to consider to apply SR-PSF to other materials such as plastic and metal in future works.

References

1) R. S. Hunter and R. W. Harold, "The Measurement of Appearance 2nd edition ," (John Wiley & Sons, 1987) p.78.
2) K. E. Torrance and E. M. Sparrow, "Theory or Off-Specular Reflection from Roughened Surfaces," Jour. Opt. Soc, 57, 9, pp. 1105-1112 (1967).
3) J. F. Blinn, "Models of Light Reflection for Computer Synthesized Pictures," Computer Graphics (Proc. SIGGRAPH), pp. 192-198 (1977).
4) R. L. Cook and K. E. Torrance, "A Reflectance Model for Computer Graphics," ACM Trans. Graph, 1, 1, pp. 7-24 (1982).
5) M. Ashikhmin, S. Premoze and P. Shirley, "A Microfacet-based BRDF Generator," Computer Graphics (Proc. SIGGRAPH), pp. 65-74 (2000).
6) Wang, J., Zhao, S., Tong, X., Snyder, J., and Guo, B., "Modeling Anisotropic Surface Reflectance with Example-Based Microfacet Synthesis", ACM Transactions on Graphics, pp. 1-9, (2008).
7) Matusik, W., Pfister, H., Brand, M., and McMillan, L., "Efficient Isotropic BRDF Measurement", Proc.Eurographics Symposium on Rendering, pp. 241-247, (2003).
8) Gardner, A., Tchou, C., Hawkins, T., and Debevec, P., "Linear Light Source Reflectometry", ACM Transactions on Graphics 22, 3, pp. 749-758, (2003).
9) Ren, P., Wang, J., Snyder, J., Tong, J. X., and Guo, B., "Pocket Reflectometry", ACM Transactions on Graphics 30, 4, pp. 45:1-45:10, (2011).
10) Wang, C.-P., Snavely, N., and Marshner, S., "Estimating Dual-scale Properties of Glossy Surfaces from Step-edge Lighting", ACM Transactions on Graphics 30, 6, pp. 172:1-172:12, (2011).
11) Aittala, M., Weyrich, T., and Lehtinen, J., "Practical SVBRDF Capture In The Frequency Domain", ACM Transactions on Graphics 32, 4, (2013).
12) M. Lindstrand, "Instrumental Gloss Characterization – In the Light of Visual Evaluation: A Review," J. Imaging Sci. Technol., 49, 1, pp. 61-70 (2005).
13) R. W. Fleming, "Visual Perception of Materials and Their Properties," Vision Research, 94, pp. 62-75 (2014).
14) Inoue S., and Tsumura, N., "Relationship between PSF and Goniorefreflectance distribution of Specular Reflection", Proc. CGIV, pp.301-306, (2012).
15) Inoue, S., Kotori, Y., and Takishiro, M., "Measurement Method for PSF of Paper on Specular Reflection Phenomenon (Part I) ", JAPAN TAPPI JORNAL, 66, 8, pp.871-886, (2012).
16) Inoue, S., Kotori, Y., and Takishiro, M., "Measurement Method for PSF of Paper on Specular Reflection Phenomenon (Part II) ", JAPAN TAPPI JORNAL, 66, 12, pp.1425-1434, (2012).
17) James, T.H., "The Theory of the Photographic Process", pp.592-635, (1977).
18) Inoue, S., Tsumura, N., and Miyake, Y., "Measuring MTF of Paper by Sinusoidal Test Pattern Projection", J. Imaging Sci. Technol., 41, 6, pp.657-661, (1997).
19) Rogers, G.L, "Measurement of the modulation transfer function of paper", Appl. Opt., 37, 31, pp.7235-7240, (1998).
20) Takano, R., Baba, K., Inoue, S., Miyata, K., and Tsumura, N., "Reproduction of Gloss Unevenness on Printed Paper by Reflection Model with Consideration of Mesoscopic Facet", Proc. CIC, pp.206-210, (2012).
21) ISO 8254-1:2009 TAPPI method: Paper and board - Measurement of specular gloss - Part 1: 75 degree gloss with a converging beam, www.iso.org.